6

Influence of Thickness on Structural and Optical Properties of Titanium Oxide Thin Layers

Haleh Kangarlou[1] and Saeid Rafizadeh[2]
[1]*Faculty of Science, Urmia Branch, Islamic Azad University, Urmia*
[2]*Faculty of Engineering, Urmia Branch, Islamic Azad University, Urmia*
Iran

1. Introduction

Many researchers have reported on obtaining TiO_2 thin films, using different methods [1-7]. These extensive studies on TiO_2 have been due to the importance of these films in variety of applications including low-loss, low-scatter optical coating for visible and near infrared optics [8-11] and electrical devices [12,13]. These applications have stimulated a considerable amount of activity in fabrication of dielectric films with high refractive index and low absorption. Compact thin films of TiO_2 on conducting glass are used in new types of solar cells: liquid and solid dye-sensitized photo-electrochemical solar cells [14,15]. These films are also of interest for the photo-oxidation of water [16], photo-catalytisis [17], electro chromic devices [18] and other uses [19]. Due to the need of cost competitive devices in these application areas, simple and inexpensive techniques are required for film deposition and preparation.

Different properties of thin films are strongly influenced by the nanostructure of films such as grain sizes, nano-strain, crystallographic orientation and other features. It is shown that nanostructure of thin films are strongly affected by film preparation procedures and deposition conditions. For example, the substrate temperature [20-22], angle of incidence [23-25], deposition rate [26,27], and film thickness [28] have important effects on the morphology and nanostructure of thin films. Some synthetic methods for TiO_2 nanostructures are:

1.1 Sol-gel method

In a typical sol-gel process, a colloidal suspension, or a sol, is formed from the hydrolysis and polymerization reactions of the precursors, which are usually inorganic metal salts or metal organic compounds such as metal alkoxides.

TiO_2 nanomaterials have been synthesized with the sol-gel method from hydrolysis of a titanium precursor. This process normally proceeds via an acid-catalyzed hydrolysis step of titanium(IV) alkoxide followed by condensation. The development of Ti-O-Ti chains is favored with low content of water, low hydrolysis rates, and excess titanium alkoxide in the reaction mixture. Three-dimensional polymeric skeletons with close packing result from the development of Ti -O- Ti chains. The formation of $Ti(OH)_4$ is favored with high hydrolysis rates for a medium amount of water. The presence of a large quantity of Ti-OH and

insufficient development of three-dimensional polymeric skeletons lead to loosely packed first-order particles. Polymeric Ti -O- Ti chains are developed in the presence of a large excess of water. Closely packed first-order particles are yielded via a three-dimensionally developed gel skeleton. From the study on the growth kinetics of TiO_2 nanoparticles in aqueous solution using titanium tetraisopropoxide (TTIP) as precursor, it is found that the rate constant for coarsening increases with temperature due to the temperature dependence of the viscosity of the solution and the equilibrium solubility of TiO_2. Secondary particles are formed by epitaxial self-assembly of primary particles at longer times and higher temperatures, and the number of primary particles per secondary particle increases with time. The average TiO_2 nanoparticle radius increases linearly with time, in agreement with the Lifshitz-Slyozov-Wagner model for coarsening.

A series of thorough studies have been conducted by Sugimoto et al. using the sol-gel method on the formation of TiO_2 nanoparticles of different sizes and shapes by tuning the reaction parameters Typically, a stock solution of a 0.50 M Ti source is prepared by mixing TTIP with triethanolamine (TEOA) ([TTIP]/[TEOA] = 1:2), followed by addition of water. The stock solution is diluted with a shape controller solution and then aged at 100 °C for I day and at 140 °C for 3 days. The pH of the solution can be tuned by adding $HCI0_4$ or NaOH solution. Amines are used as the shape controllers of the TiO_2 nanomaterials and act as surfactants. These amines include TEOA, diethylenetriamine, ethylenediamine, trimethylenediamine, and triethylenetetramine.

By a combination of the sol-gel method and an anodic alumina membrane (AAM) template, TiO_2 nanorods have been successfully synthesized by dipping porous AAMs into a boiled TiO_2 sol followed by drying and heating processes. [38]

1.2 Micelle and inverse micelle methods

Aggregates of surfactant molecules dispersed in a liquid colloid are called micelles when the surfactant concentration exceeds the critical micelle concentration (CMC). The CMC is the concentration of surfactants in free solution in equilibrium with surfactants in aggregated form. In micelles, the hydrophobic hydrocarbon chains of the surfactants are oriented toward the interior of the micelle, and the hydrophilic groups of the surfactants are oriented toward the surrounding aqueous medium. The concentration of the lipid present in solution determines the self-organization of the molecules of surfactants and lipids. The lipids form a single layer on the liquid surface and are dispersed in solution below the CMC. The lipids organize in spherical micelles at the first CMC (CMC-I), into elongated pipes at the second CMC (CMC-II), and into stacked lamellae of pipes at the lamellar point (LM or CMC-III). The CMC depends on the chemical composition, mainly on the ratio of the head area and the tail length. Reverse micelles are formed in nonaqueous media, and the hydrophilic head groups are directed toward the core of the micelles while the hydrophobic groups are directed outward toward the nonaqueous media. There is no obvious CMC for reverse micelles, because the number of aggregates is usually small and they are not sensitive to the surfactant concentration. Micelles are often globular and roughly spherical in shape, but ellipsoids, cylinders, and bilayers are also possible. The shape of a micelle is a function of the molecular geometry of its surfactant molecules and solution conditions such as surfactant concentration, temperature, pH, and ionic strength. [38]

1.3 Sol method

The sol method here refers to the nonhydrolytic sol-gel processes and usually involves the reaction of titanium chloride with a variety of different oxygen donor molecules, e.g., a metal alkoxide or an organic ether.

$$Ti\ X_4 + Ti(OR)_4 \rightarrow 2TiO_2 + 4RX \quad (1)$$

$$TiX_4 + 2ROR \rightarrow TiO_2 + 4RX \quad (2)$$

The condensation between Ti-CI and Ti-OR leads to the formation of Ti-O-Ti bridges. The alkoxide groups can be provided by titanium alkoxides or can be formed in situ by reaction of the titanium chloride with alcohols or ethers. In the method by Trentler and Colvin, a metal alkoxide was rapidly injected into the hot solution of titanium halide mixed with trioctylphosphine oxide (TOPO) in heptadecane at 300 °C under dry inert gas protection, and reactions were completed within 5 min. For a series of alkyl substituents including methyl, ethyl, isopropyl, and tert-butyl, the reaction rate dramatically increased with greater branching of R, while average particle sizes were relatively unaffected. Variation of X yielded a clear trend in average particle size, but without a discernible trend in reaction rate. Increased nucleophilicity (or size) of the halide resulted in smaller anatase nanocrystals. Average sizes ranged from 9.2 nm for TiF_4 to 3.8 nm for TiI_4. The amount of passivating agent (TO PO) influenced the chemistry. Reaction in pure TOPO was slower and resulted in smaller particles, while reactions without TOPO were much quicker and yielded mixtures of brookite, rutile, and anatase with average particle sizes greater than 10 nm. [38]

1.4 Hydrothermal method

Hydrothermal synthesis is normally conducted in steel pressure vessels called autoclaves with or without Teflon liners under controlled temperature and/or pressure with the reaction in aqueous solutions. The temperature can be elevated above the boiling point of water, reaching the pressure of vapor saturation. The temperature and the amount of solution added to the autoclave largely determine the internal pressure produced. It is a method that is widely used for the production of small particles in the ceramics industry. Many groups have used the hydrothermal method to prepare TiO_2 nanoparticles. [38]

1.5 Solvothermal method

The solvothermal method is almost identical to the hydrothermal method except that the solvent used here is nonaqueous. However, the temperature can be elevated much higher than that in hydrothermal method, since a variety of organic solvents with high boiling points can be chosen. The solvothermal method normally has better control than hydrothermal methods of the size and shape distributions and the crystallinity of the TiO_2 nanoparticles. The solvothermal method has been found to be a versatile method for the synthesis of a variety of nanoparticles with narrow size distribution and dispersity. The solvothermal method has been employed to synthesize TiO_2 nanoparticles and nanorods with/without the aid of surfactants. [38]

1.6 Chemical vapor deposition

Vapor deposition refers to any process in which materials in a vapor state are condensed to form a solid-phase material. These processes are normally used to form coatings to alter the mechanical, electrical, thermal, optical, corrosion resistance, and wear resistance properties of various substrates. They are also used to form free-standing bodies, films, and fibers and to infiltrate fabric to form composite materials. Recently, they have been widely explored to fabricate various nanomaterials. Vapor deposition processes usually take place within a vacuum chamber. If no chemical reaction occurs, this process is called physical vapor deposition (PVD); otherwise, it is called chemical vapor deposition (CVD). In CVD processes, thermal energy heats the: gases in the coating chamber and drives the deposition reaction. [38]

1.7 Physical vapor deposition

In PVD, materials are first evaporated and then condensed to form a solid material. The primary PVD methods include thermal deposition, ion plating, ion implantation, sputtering, laser vaporization, and laser surface alloying. TiO2 nanowire arrays have been fabricated by a simple PVD method or thermal deposition. [38]

1.8 Electrodeposition

Electrodeposition is commonly employed to produce a coating, usually metallic, on a surface by the action of reduction at the cathode. The substrate to be coated is used as cathode and immersed into a solution which contains a salt of the metal to be deposited. The metallic ions are attracted to the cathode and reduced to metallic form. With the use of the template of an AAM, TiO_2 nanowires can be obtained by electrodeposition. [38] Optical properties of Ti thin films, despite their importance in different technologies, are only reported by Johnson and Christy [29] and for Bulk Ti samples by Lynch et al [30] and Wall et al [31].Therefore, it is of interest to find out the relationship between different theories [32-34] given for optical parameters and the structural changes described by variation of film thickness [35-37]. Accordingly, it was decided to investigate the influence of film thickness on the optical and structural properties of Titanium oxide films produced at high temperature of 473 K.

2. Experimental details

Titanium oxide films of 10, 50, 100 and 200 nm thickness were deposited by evaporation of TiO_2 powder, on glass substrates at 473 K deposition temperature. The residual gas was composed mainly of H_2, H_2O, CO and CO_2 as detected by quad ro pole mass spectrometer. The substrate normal was at 8.5 degree to the direction of evaporated beam and the distance between the evaporation crucible and substrate was 54.5 cm. Substrates were glasses (2×2×1 cm^3) of minimum roughness.

Just before use, all glass substrates were ultrasonically cleaned in heated acetone, then ethanol. The near normal incidence reflectance spectra were obtained using a double beam spectrophotometer (carry 500) in the spectral range of 200-2500 nm corresponding to the energy range of 0.6-6.215 eV.

Nanostructures of these films were obtained using a Philips XRD X pert MPD Diffractometer (CuK_α radiation) with a step size of 0.03 and count time of 1s per step, while the surface physical morphology and roughness were obtained by means of AFM (Dual Scope™DS95-200/50)analysis

3. Results and discussion

3.1 Optical constants of TiO_2 fils as a function of film thickness

Kramers-Kronig relations were used to convert the measured reflectivity spectra of complex dielectric function, from which the optical conductivity absorption coefficient and other parameters were calculated.

Figures 1(a) and 1(b), show spectra of ε_1 and ε_2 for TiO_2/glass films of different thicknesses (10 nm to 200 nm) produced at 473 K deposition temperature, respectively. Johnson and Christys results [29] for thin Ti films (30 nm) and Lynch et al results [30] for bulk Ti samples are also included for comparison. Ti is a getter metal and a rare Ti film can not be prepared even in UHV conditions. The general trend of our results is similar to those of Johnson and Christy, and Lynch et al (Figure 1(a,b)). As it can be seen in Figure 1(a), all curves begin from negative values and reach to a maximum pick at about 0.9 eV. Generally by increasing film thickness, real part of dielectric constant increases (Figure 1(a)) and that is because of producing TiO_2 dielectric layers. As it can be seen in Figure 1(b), there is a peak at about 1.5 eV for all layers. By increasing the thickness, in the energy range of 1 eV up to 4 eV, general trend of ε_2 curves increases. For the rest of energy range (4 eV up to 6 eV), there is no general trend for ε_2 curves, and that is because of competition between increasing film thickness and surface and bulk diffusion of grains at high 473 K temperature.

3.2 Effective-media appraximation (EMA) approach

The correlation between the nanostructure of TiO_2 thin film and it's optical property achieved through using the effective-media approximation (EMA) method. The changes in fraction of voids can be attributed to the change of nanostructures in the evolution of film nanostructures by substrate temperature, film thickness and deposition rate.

The effect of voids on optical properties of thin films can be investigated by the Bruggman effective-media approximation method [33] or its version developed by aspens and coworkers [32]. As it can be seen in Figure (2), by increasing film thickness, in 1 eV up to 4 eV energy range, fraction of voids decreases. For the rest of analysis range (4 eV up to 6 eV), fraction of voids due to competition between increasing film thickness and surface and bulk diffusion of grains at high 473 K temperature, cross each other. So there is a good correlation between nanostructures and optical properties in our results.

3.3 Interband region

The energy bands for TiO_2 were calculated using potential in Shroudinger equation. The obtained experimental absorption coefficients ($\alpha=2Ek/hc$) for TiO_2 films, were plotted in Figure (3). The plots have a good agreement with those of Janson and Cheristy and Lynch et al. In general by increasing film thickness, absorption coefficient also increases. By increasing the thickness, fraction of voids decreases, specially in the energy renge of

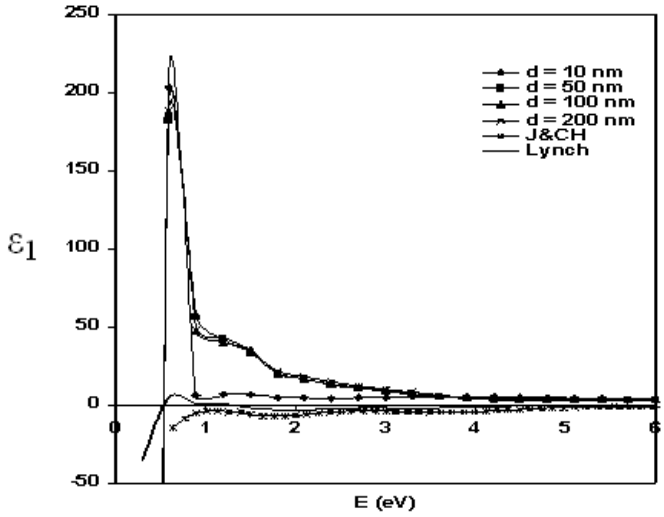

(a)

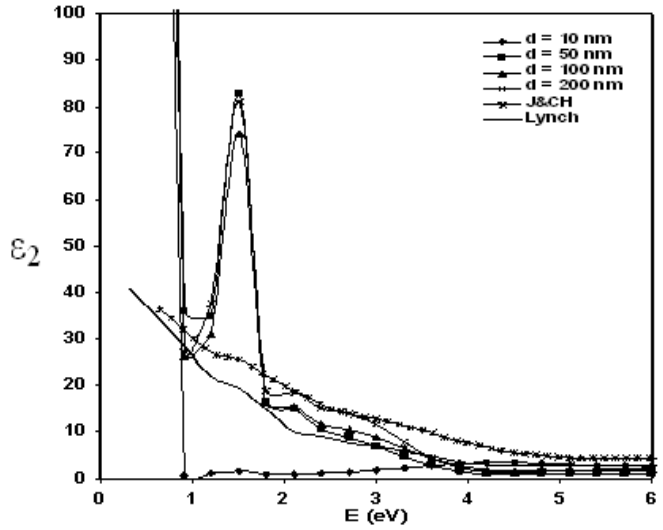

(b)

Fig. 1. The dielectric constants of deposited TiO_2/glass films of Different thicknesses at 473 k (a) Real port (b) Imaginary Port.

1 eV – 4 eV, which is in agreement with fraction of voids (Figure 2). In the energy renge of 1 eV - 4 eV, transmittance decreases and absorbance increases. In the energy renge of 4 eV - 6 eV, there is no general trend for absorption coefficient curves and they cross each other. That is because of competition between surface and bulk diffusion in one hand and increasing thickness on the other hand. This result is also in agreement with EMA results. There was an inter band transition at energy value of about 4.5 eV.

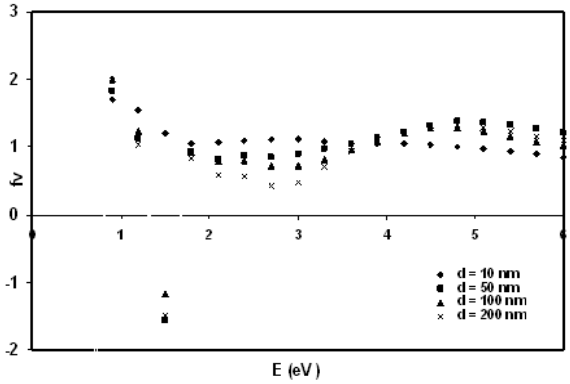

Fig. 2. Void fraction Vs. energy for different film thicknesses deposited TiO_2/glass films at 473 k.

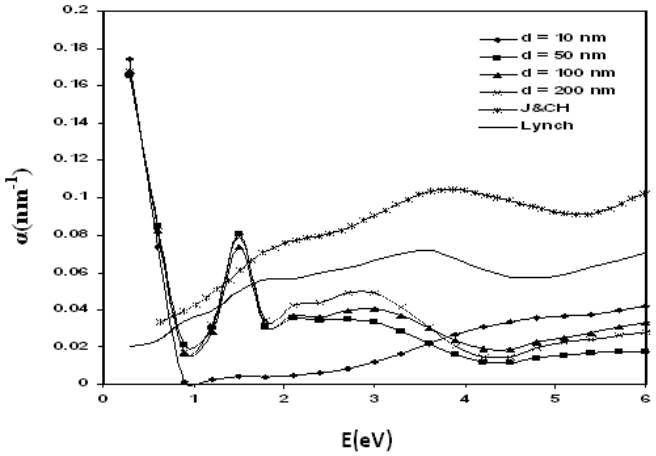

Fig. 3. Absorption coefficient vs. energy for different film thicknesses deposited TiO_2/glass films at 473 k.

Transmission spectroscopy was used to study optical properties of thin TiO_2 films. It was found that, low independent transmission absorbance measurements of a thin film, if the thickness is unknown, are sufficient for numerical inversion to determine the complex index of refraction of a film. Real part of refractive index (n) and imaginary part of refractive index (k) are shown in Figure 4 (a) and (b) respectively. As it can be seen in Figures 4(a) and 4(b), by increasing film thickness, general trend of the curves increases. 10 nm thickness is very thin so produced layer is uncompleted and we expect unusual behavior. By increasing thickness at high temperature (473 K), because of surface and bulk diffusion bigger grains form (will be discus in AFM analysis), that tends to increase refractive indexes (Figure 4(a)). Also by increasing thickness at high temperature (473 K), due to migration of grains, fraction of voids decreases, which results in, less transmittance as well as an increase in imaginary part of refractive index (k), see Figure 4 (b).

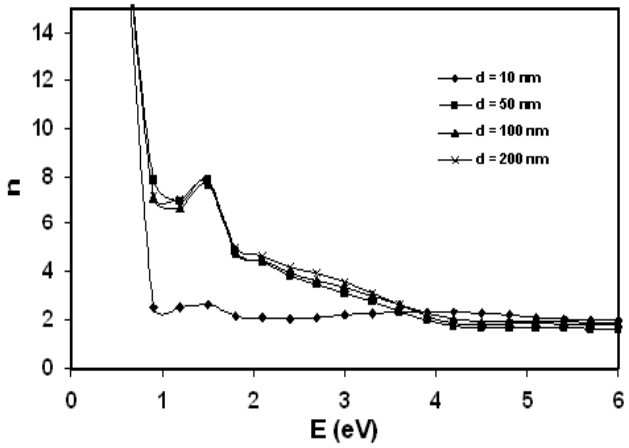

(a)

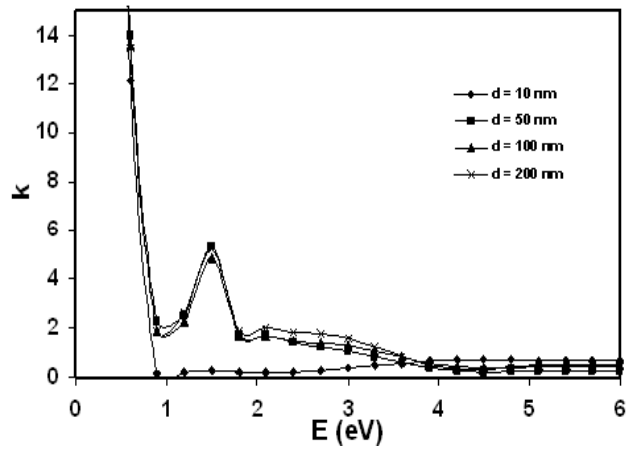

(b)

Fig. 4. Refractive index Vs. energy for different film thicknesses deposited TiO_2/glass films at 473 k,(a) Real part (b) Imaginary part.

3.4 AFM analaysis

Figure 5, shows the AFM images of TiO_2 / glass layers of different thicknesses at 473 k temperature. Figure 5(a), shows topography of TiO_2 / glass of 10 nm thickness. As it can be seen there are small grains on surface and the film surface is almost the same as substrate. By increasing thickness to 50 nm and in presence of 473 K temperature, surface diffusion happens and it forms bigger grains with small grains between them (Figure 5(b)). By increasing thickness to 100 nm in Figure 5 (c), most of the holes are covered with metallic grains and smoother layer produces and by increasing thickness to 200 nm, due to surface and bulk diffusion, domed grains appear (Figure 5(d)). By increasing thickness at high temperature, needle like and small grains change to big and domed grains.

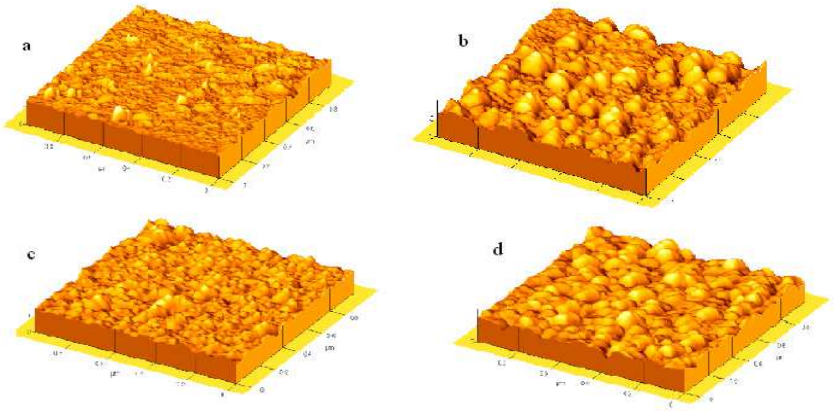

Fig. 5. The topography of TiO_2 / glass with (a)10 nm, (b)50 nm, (c)100 nm, (d)200 nm thickness at 473 k.

3.5 Roughness

Figure (6), shows the roughness curve of produced layers. As it can be seen by increasing thickness to 50 nm, roughness increases. At 100 nm and 200 nm thickness, due to surface and bulk diffusion and coalescence of grains, a decrease in fraction of voids happens (as discussed in optical properties) and roughness decreases. Generally by increasing thickness in high temperature almost roughness decreases.

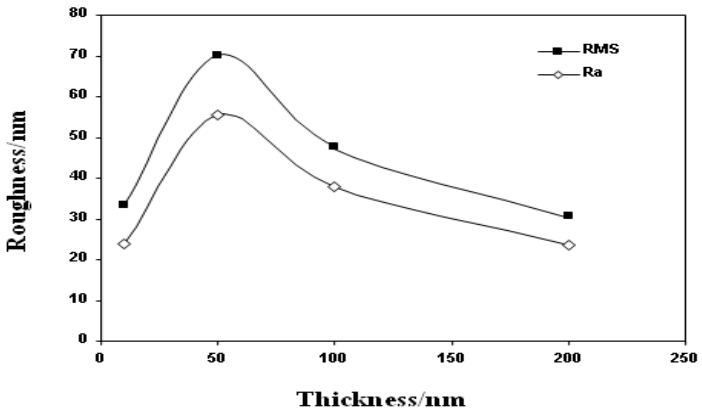

Fig. 6. The roughness curve of produced TiO_2 / glass layers at 473 k.

3.6 XRD analysis

Figure (7), shows the XRD patterns of produced layers. As it can be seen in Figure 7(a), for the layer of 10 nm thickness, no clear peak is appeared so the layer is amorphous. By increasing thickness to 50 nm, TiO_2 layer is getting crystallized and anatase A(200) crystallographic direction begin to grow (Figure 7 (b)). By increasing the thickness to 100 nm

and 200 nm (Figure 7(c) and 7(d)), layers are crystallized and anatas A(004) crystallographic direction appear. By increasing thickness the pick becomes sharper. High temperature and thickness play an important role on the layers crystallization.

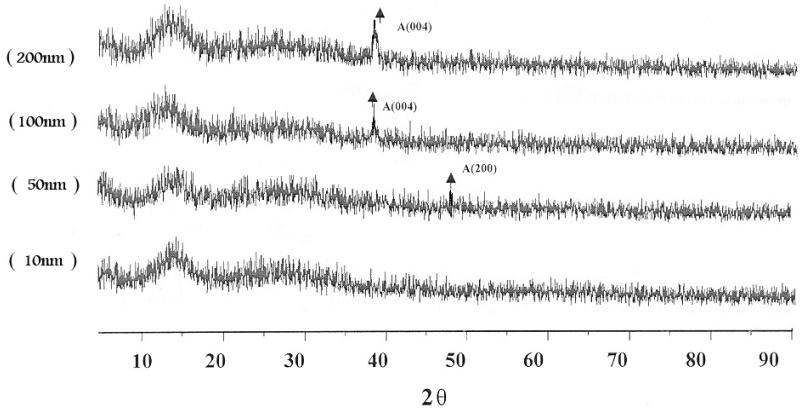

Fig. 7. The XRD pattern of TiO_2 / glass layers with different thicknesses at 473 k.

3.7 AFM Analaysis of other samples

Figure 8(a-d), shows AFM images of different thicknesses 20 nm, 70 nm, 200 nm and 250 nm respectively in presence of 600 K annealing temperature and Oxygen flow. As it can be seen heat and oxygen have different effects on different thicknesses. Morphology of these layers are completely different. For thinner layers (Figure 8(a) and 8(b)), Oxygen penetrate to

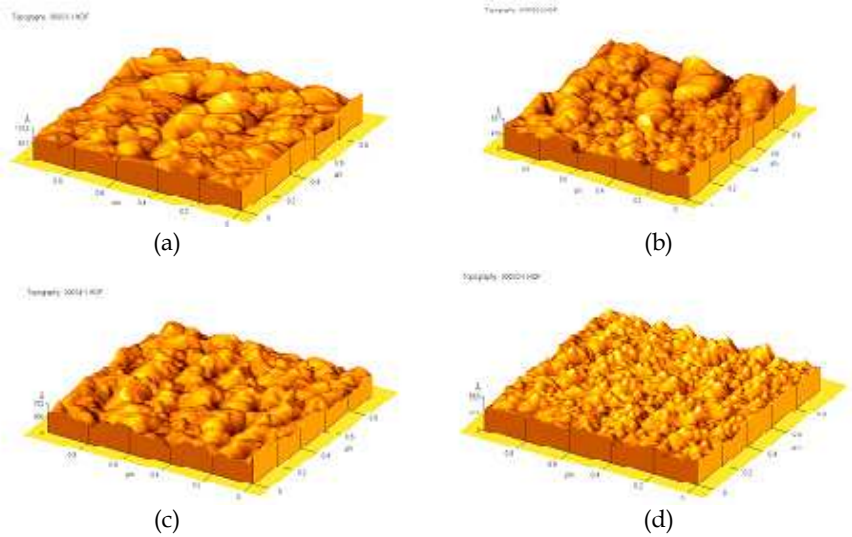

Fig. 8. The topography of TiO_2 / glass with (a)20 nm, (b)70 nm, (c)200 nm, (d)250 nm thickness at 600 k.

depth of the layers and by exerting high temperature, coalescence of grains happen and big domed grains appear. For thicker layers of 200 nm and 250 nm layers (Figure 8(c) and 8(d)), it seems that oxygen is penetrating to a special depth of surface and by exerting heat coalescence happens but grains are smaller in comparison with thinner layers. It was found that, film thickness play an important role on nanostructures of produced thin layers.

4. Conclusion

The relationship between nanostructure of TiO_2 thin films of different thicknesses (10 nm to 200 nm) produced at 473 K deposition temperature were studied. Optical properties, topography, roughness and crystallization of these films were investigated. Optical properties were investigated by studying the relationship between nanostructure and EMA, while the EMA results were dependent on dielectric constant of both film and bulk samples. The optical constants of the films were effected by the film thickness and high deposition temperature. By increasing film thickness, dielectric constants, absorption coefficient and real and imaginary parts of refractive indexes increased. Almost for all plots of 4 eV - 6 eV energy range, curves cross each other, that is because of competition between surface and bulk diffusion in one hand and increasing thickness on the other hand. The fraction of voids were obtained using the EMA method. The deviation from a general increasing or decreasing trend is due to the competition between surface and bulk diffusion of grains and film thickness. The results of absorption coefficient versus photon energy in inter band region for TiO_2 films were found to fall into a band, which is confined by Johnson and Christy's results (for thin film) at the top of band and those of Lynch et al (bulk Ti sample) at the bottom.

Topography of layers showed that, by increasing thickness at high temperature (473 K), surface and bulk diffusion happened and changed the shape of grains. Roughness curve showed that only for 50 nm thickness, roughness increased but for 100 nm and 200 nm due to surface and bulk diffusion and migration of the grains, roughness decreased.

XRD pattern of the layers showed that the 10 nm TiO_2 layer is amorphous and by increasing thickness, layers become crystallized. Crystallographic direction as A (200) for 50 nm and A(004) for 100 nm and 200 nm TiO_2 layers, appeared. By increasing thickness A(004) peak become sharper.

Finally the AFM images of another samples of 20 nm, 70 nm, 200 nm and 250 nm thicknesses deposited at 600 k were studied and it was found that, film thickness play an important role on nanostructures of produced thin layers.

5. References

[1] L. Kavan, M. Gratzel, Electrochim. *Acta*, 40 (1995) 643.
[2] S. D. Burnside, V. Shklover, C. Barbe, *Chem. Mater*., 10 (1998) 2419.
[3] P. Sawunyyama, A. Yasumori,m K. Okada, *Mater. Res. Bull*., 33 (1998) 795.
[4] S. Deki, Y. Aoi, *J. Mater. Res*. 13 (1998) 883.
[5] S. Yin, Y. Inoue, S. Uchida, Y. Fujishiro, T. Sato, *J. Mater. Res*., 13 (1998) 844.

[6] E. Vigil, L. Saadoun, R. Rodriguez-Clemente, J. A. Ayllon, X. Domenech, *J.Mater. Sci. Lett*., 18 (1999) 1067.
[7] H. Savaloni, K. Khojier, M. S. Alaee, *J. Mater. Sci*., 42 (2007) 2603.
[8] K. A. Vorotilov, E. V. Orlova, V. I. Petrovsky, *Thin Solid Films*, 207 (1992) 180.
[9] M. G. Krishana, K. Narasimaha Rao, S. Mohan, *J. Appl. Phys*., 73 (1983) 434.
[10] J. Rancourt, *User's Handbook: Optical Thin Film, McGrow-Hill*, New York, 1987.
[11] J. A. Dobrowski, in: W. Driscoll (Ed.), *Coating and Filters in Handbook of Optics, MacGrow-Hill*, New York, 1987.
[12] P. Babelon, A. S. Dequiedt, H. Mostesa-Sba, S. Bourgeois, P. Sibillot, M. Sacilotti, *Thin Solid Films*, 322 (1998) 63.
[13] Y. Leprince-Wang, K.-Y. Zhang, V. Nguyen, V. An, D. Souche, J. Rivory, *Thin Solid Films*, 307 (1997) 38.
[14] B. O'Regan, M. Gratzel, *Nature*, 353 (1991) 737.
[15] U. Bach, D. Lupo, P. Comte, J. E. Moser, F. Weissortel, J. Salbeck, H. Spreitzer,M. Gratzel, *Nature*, 395 (1998) 583.
[16] L. Kavan, M. Gratzel, Electrochim. *Acta*, 40 (1995) 643.
[17] R. L. Pozzo, M. A. Baltanas, A. E. Cassano, *Catalysis Today*, 39 (1997) 219.
[18] T.-S. Kang, D. Kim, K.-J. Kim, *J. Electrochem. Soc*., 145 (1998) 1982.
[19] Y. Paz, Z. Luo, L. Rabenberg, A. Heller, *J. Mater. Res*., 10 (1995) 2842.
[20] Ida, T.& Toraya, H., *J. Appl. Cryst*. 35 (2002) 58.
[21] M. Cernasky, *J. Appl. Cryst*. 16 (1983) 103.
[22] R. W. Cheary and A. Coelho, *J. Appl. Cryst*. 25 (1992) 109.
[23] D.Balzar and S.Popovic, *J. Appl. Cryst*. 29 (1996) 16.
[24] D.Balzar, *J. Appl. Cryst*. 25 (1992) 559.
[25] J. K. Yau and S. A. Howard, *J. Appl. Cryst*. 22 (1989) 244.
[26] S. A. Howard, and R. L. Snyder, *J. Appl. Cryst*. 22 (1989) 238.
[27] S. Enzo, G. Fagherazzi, A. Benedetti and S. Polizzi, *J. Appl. Cryst*. 22 (1989) 184.
[28] H. Savaloni, A. Taherizadeh, A. Zendehnam, *Physica B*, 349 (2004) 44.
[29] R. B. Johnson and R. W. Christy, *Physical Review B*, 9 (1974) 5056.
[30] D. W. Lynch, C. G. Olson, J. H. Weaver, *Physical Review B*, 11 (1975) 3617.
[31] W. E. Wall, M. W. Ribrasky and J. R. Stevenson, *J. App. Phys*, 51 (1980) 661.
[32] E. Aspnes, *Thin Solid Films*, 89 (1982) 249.
[33] D. A. G. Brauggeman, *Ann. Phys. (Leipzig)*, 24 (1935) 636.
[34] E. Aspnes, E. Kinsbron, and D. D. Bacon, *Phys. Rev*. B21 (1980) 3290.
[35] R. Messier and J. E. Yahoda, J. *Appl. Phys*, 58 (1985) 3739.
[36] P. B. Barna, M. Adamik, *Thin Solid Films*, 317 (1998) 27.
[37] Petrov, P. B. Barna, L. Hultman, J. E. Greene, *J. Vac.Sci. Technol*,S117-S128.
[38] Xiaobo Chen and Samuel S. Mao, *Chem. Rev*. 2007, 107, 2891-2959.

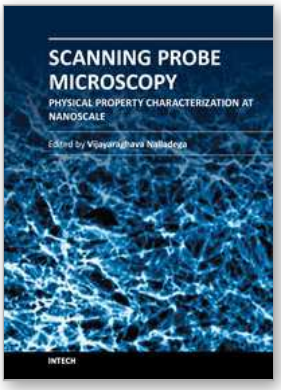

Scanning Probe Microscopy-Physical Property Characterization at Nanoscale

Edited by Dr. Vijay Nalladega

ISBN 978-953-51-0576-3
Hard cover, 242 pages
Publisher InTech
Published online 27, April, 2012
Published in print edition April, 2012

Scanning probe microscopy (SPM) is one of the key enabling tools for the advancement for nanotechnology with applications in many interdisciplinary research areas. This book presents selected original research works on the application of scanning probe microscopy techniques for the characterization of physical properties of different materials at the nanoscale. The topics in the book range from surface morphology analysis of thin film structures, oxide thin layers and superconducting structures, novel scanning probe microscopy techniques for characterization of mechanical and electrical properties, evaluation of mechanical and tribological properties of hybrid coatings and thin films. The variety of topics chosen for the book underlines the strong interdisciplinary nature of the research work in the field of scanning probe microscopy.

How to reference

In order to correctly reference this scholarly work, feel free to copy and paste the following:

Haleh Kangarlou and Saeid Rafizadeh (2012). Influence of Thickness on Structural and Optical Properties of Titanium Oxide Thin Layers, Scanning Probe Microscopy-Physical Property Characterization at Nanoscale, Dr. Vijay Nalladega (Ed.), ISBN: 978-953-51-0576-3, InTech, Available from: http://www.intechopen.com/books/scanning-probe-microscopy-physical-property-characterization-at-nanoscale/influence-of-thickness-on-structural-and-optical-properties-of-titanium-oxide-thin-layers

INTECH
open science | open minds

InTech Europe
University Campus STeP Ri
Slavka Krautzeka 83/A
51000 Rijeka, Croatia
Phone: +385 (51) 770 447
Fax: +385 (51) 686 166
www.intechopen.com

InTech China
Unit 405, Office Block, Hotel Equatorial Shanghai
No.65, Yan An Road (West), Shanghai, 200040, China
中国上海市延安西路65号上海国际贵都大饭店办公楼405单元
Phone: +86-21-62489820
Fax: +86-21-62489821